AN ALTERNATIVE COARSE SPACE FOR IRREGULAR SUBDOMAINS AND AN OVERLAPPING SCHWARZ ALGORITHM

CLARK R. DOHRMANN[*] AND OLOF B. WIDLUND[†]

TR2011-946

Abstract. In earlier work on domain decomposition methods for elliptic problems in the plane, an assumption that each subdomain is triangular, or a union of a few coarse triangles, has often been made. This is similar to what is required in geometric multigrid theory and is unrealistic if the subdomains are produced by a mesh partitioner. In an earlier paper, coauthored with Axel Klawonn, the authors introduced a coarse subspace for an overlapping Schwarz method with one degree of freedom for each subdomain vertex and one for each subdomain edge. A condition number bound proportional to $(1 + \log(H/h))^2(1 + H/\delta)$ was established assuming only that the subdomains are John domains; here H/δ measures the relative overlap between neighboring subdomains and H/h the maximum number of elements across individual subdomains. We were also able to relate the rate of convergence to a parameter in an isoperimetric inequality for the subdomains into which the domain of the problem has been partitioned.

In this paper, the dimension of the coarse subspace is decreased by using only one degree of freedom for each subdomain vertex; if all subdomains have three edges, this leads to a reduction of the dimension of the coarse subspace by approximately a factor four. In addition, the condition number bound is shown to be proportional to $(1 + \log(H/h))(1 + H/\delta)$ under a quite mild assumption on the relative length of adjacent subdomain edges.

In this study, the subdomains are assumed to be uniform in the sense of Peter Jones. As in our earlier work, the results are insensitive to arbitrary large jumps in the coefficients of the elliptic problem across the interface between the subdomains.

Numerical results are presented which confirm the theory and demonstrate the usefulness of the algorithm for a variety of mesh decompositions and distributions of material properties. It is also shown that the new algorithm often converges faster than the older one in spite of the fact that the dimension of the coarse space has been decreased considerably.

Key words. domain decomposition, elliptic equations, overlapping Schwarz preconditioners, coarse subspaces, irregular subdomain boundaries, discontinuous coefficients

AMS subject classifications. 35Q60, 65F10, 65N30, 65N55

1. Introduction. We will consider scalar elliptic problems in the plane of the form

$$-\nabla \cdot (\rho(x)\nabla u(x)) \;=\; f(x), \;\; x \in \Omega \subset \mathbb{R}^2, \tag{1.1}$$

with a zero Dirichlet boundary condition on a subset $\partial\Omega_D$ of $\partial\Omega$, the boundary of Ω, and a Neumann condition on $\partial\Omega_N = \partial\Omega \setminus \partial\Omega_D$. We can for example assume that $\partial\Omega_D$ contains at least one edge of one subdomain.

The domain Ω is decomposed into N non-overlapping subdomains $\Omega_1, \ldots, \Omega_N$. The coefficient $\rho(x)$ is strictly positive and assumed to be a constant ρ_i for $x \in \Omega_i$. We will use a variational formulation of the elliptic problem, written in terms of

bilinear forms associated with these subdomains:

$$a(u,v) \; := \; \sum_{i=1}^{N} a_i(u,v) \; := \; \sum_{i=1}^{N} \rho_i \int_{\Omega_i} \nabla u \cdot \nabla v dx. \tag{1.2}$$

Each Ω_i is simply connected and has a connected boundary $\partial\Omega_i$. The subdomains can have quite irregular boundaries; see Definition 2.1 of *uniform domains.*

We denote by $H_i = \text{diameter}(\Omega_i)$. The *interface* of this decomposition is given by

$$\Gamma := \left(\bigcup_{i=1}^{N} \partial\Omega_i \right) \backslash \partial\Omega_D,$$

and the contribution to Γ from $\partial\Omega_i$ by $\Gamma_i := \partial\Omega_i \setminus \partial\Omega_D$. These sets are unions of subdomain edges and vertices. The subdomain edge $\mathcal{E}^{ij}$ common to Ω_i and Ω_j is typically defined as $\partial\Omega_i \cap \partial\Omega_j$ but excluding the two subdomain vertices at its endpoints. The intersection of the two subdomain boundaries might have several components. In such a case, each such component will be regarded as an edge; this will not cause any extra complications. The set of all subdomain edges are denoted by $\mathcal{S}_\mathcal{E}$ and the set of those belonging to Γ_i by $\mathcal{S}_{\mathcal{E}_i}$. Similarly, the set of all subdomain vertices will be denoted by $\mathcal{S}_\mathcal{V}$ and those on Γ_i by $\mathcal{S}_{\mathcal{V}_i}$.

We use piecewise linear, continuous finite elements and triangulations with shape regular elements and assume that each subdomain is the union of a set of elements with all nodes matching across the interface. The smallest element diameter of the elements of $\mathcal{T}_{h_i}$, the triangulation of Ω_i, is denoted by h_i and the smallest angle in this triangulation is assumed to be bounded from below by a mesh independent positive constant. The conforming finite element space of piecewise linear, continuous functions associated with the triangulation of Ω will be denoted by V^h. We could equally well develop our algorithm and theory for any other conforming, low order elements on triangular or quadrilateral meshes.

The nodal finite element interpolant of a sufficiently smooth function $u \in H^1(\Omega_i)$ is defined as

$$I^{h_i}(u) := \sum_{v \in \mathcal{N}^{h_i}} u(v)\phi_v, \tag{1.3}$$

where $\mathcal{N}^{h_i}$ is the set of nodes of $\mathcal{T}_{h_i}$, $u(v)$ is the value of u at node v, and $\phi_v \in H^1(\Omega_i)$ is the shape function for node v. A coarse interpolant of u will be introduced in Definition 2.6 and further considered in Lemmas 2.7 and 2.9.

Our current work follows earlier work on the effects of irregular subdomains on the performance of different domain decomposition algorithms; see [3, 4, 5, 7, 11]. At the core of the present study are coarse space basis functions associated with the subdomain vertices. They were originally developed in a comprehensive study of H(curl) problems in the plane, see [7], but were not included in the final paper. In this paper, they serve as basis functions for the coarse subspace of our overlapping Schwarz algorithm. Not only are we able to improve the bound of the condition number in comparison with that in our earlier paper [4], but the coarse subspace dimension will now equal the number of subdomain vertices rather than the number of subdomain edges and vertices. Thus, the dimension of the new coarse subspace is the same as for BDDC and FETI-DP algorithms using the standard set of primal constraints associated with the subdomain vertices, known to work well for problems in two

dimensions; see, e.g., [11]. We note that in our estimate for the coarse interpolant needed in our Schwarz analysis, we will use a bound on the energy of the coarse basis functions, given by Lemma 2.7, as well as a discrete Sobolev inequality, given by Lemma 2.8. Our estimate of the condition number of our algorithm will include a factor $(1 + \log(H/h))$; to our knowledge, no results, which are valid for arbitrary jumps in the coefficients across the interface, have been established for any domain decomposition algorithm without such a logarithmic factor.

Finally, we note that the present study is part of a larger research effort to make domain decomposition solvers more efficient and to provide full theoretical support for work on irregular shaped subdomains. Indeed, extensions of the ideas presented here have already made their way into a solver used by a massively parallel structural dynamics code [6, 1].

2. Technical tools. The results presented in this section will be used in the proof of our main result, Theorem 3.1.

Our results apply to subdomains that are *uniform.* According to Jones [9], these domains form the largest family for which a bounded extension of $H^1(\Omega_i)$ to $H^1(\mathbb{R}^2)$ is possible. We note that a uniform domain need not have a uniformly Lipschitz continuous boundary. Thus, snowflake domains (see, e.g., Figs. 5.1 and 5.3 of [4]) with fractal boundaries are in this class.

DEFINITION 2.1. *(Uniform Domain). A bounded domain $\Omega \subset \mathbb{R}^n$ is uniform if there exists a constant $C_U(\Omega) > 0$ such that for any pair x, y of points in the closure of Ω, there is a curve $\gamma(t) : [0, \ell] \to \Omega$, parametrized by arc length, such that $\gamma(0) = x$, $\gamma(\ell) = y$,*

$$\ell \ \leq \ C_U(\Omega)|x - y|, \quad and \tag{2.1}$$
$$\min(t, \ell - t) \ \leq C_U(\Omega) \cdot dist(\gamma(t), \partial\Omega). \tag{2.2}$$

REMARK 1. *There are several alternative and equivalent definitions. Thus, the left hand side of (2.2) can be replaced by*

$$\min(|\gamma(t) - x|, |\gamma(t) - y|) \quad or \ by \quad \frac{|\gamma(t) - x||\gamma(t) - y|}{|x - y|}.$$

Any good result on the convergence of a domain decomposition algorithm with two or more levels requires the use of

LEMMA 2.2. *(Poincaré's Inequality) Consider a domain $\Omega \subset \mathbb{R}^2$. Then,*

$$\|u - \bar{u}_\Omega\|_{L^2(\Omega)}^2 \leq (\gamma(\Omega, 2))^2 |\Omega| \|\nabla u\|_{L^2(\Omega)}^2, \quad \forall u \in H^1(\Omega).$$

This is [4, Lemma 2.2], $\bar{u}_\Omega$ is the average of the scalar function u over Ω, and $\gamma(\Omega, 2)$ a parameter in an isoperimetric inequality; cf. [12] or [4, Lemma 2.1]. Since any simply connected uniform domain is a John domain and, according to [2], any John domain in the plane has a finite $\gamma(\Omega, 2)$, we can use Poincaré's inequality for any uniform subdomain.

ASSUMPTION 1. *The subdomains Ω_i are all uniform domains and their uniformity constants $C_U(\Omega_i)$ are uniformly bounded from above by a mesh independent constant C_U. We also assume that $|\mathcal{S}_{\mathcal{E}_i}|$ is uniformly bounded.*

Let $\boldsymbol{d}_{\mathcal{E}}$ denote a unit vector in the direction from one endpoint of a subdomain edge $\mathcal{E}$ to the other with the same sense of direction as $\boldsymbol{t}_i$, the unit tangential vector
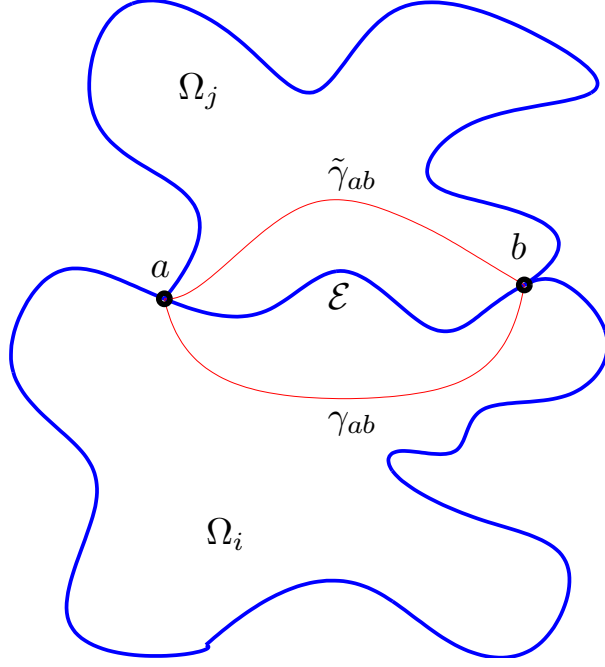
FIG. 2.1. *Figure showing geometry of an edge $\mathcal{E} = \mathcal{E}^{ij}$. The distance between the edge endpoints a and b is denoted by $d_{\mathcal{E}}$.*

of $\partial\Omega_i$, directed in a counterclockwise sense. The distance between the two endpoints of $\mathcal{E}$ is denoted by $d_{\mathcal{E}}$. Thus, $d_{\mathcal{E}}\boldsymbol{d}_{\mathcal{E}}$ is the vector from one endpoint of the subdomain edge to the other.

DEFINITION 2.3. *Let a and b denote the two endpoints of an edge $\mathcal{E} = \mathcal{E}^{ij} \in \mathcal{S}_{\mathcal{E}_i}$. The region $R_{\mathcal{E}}$ is defined as the open set with boundary*

$$\partial R_{\mathcal{E}} = \gamma_{ab}(t) \cup \mathcal{E},$$

where $\gamma_{ab}(t)$ is the curve $\gamma(t)$ in Definition 2.1 for Ω_i with $x = a$ and $y = b$.

The following result is [7, Lemma 3.4]:

LEMMA 2.4. *For the region $R_{\mathcal{E}}$ of Definition 2.3, it holds*

$$|R_{\mathcal{E}}| \leq (C_U^2/\pi)d_{\mathcal{E}}^2, \tag{2.3}$$
$$diam(R_{\mathcal{E}}) \leq (2C_U - 1)d_{\mathcal{E}} \tag{2.4}$$

where $|R_{\mathcal{E}}|$ is the area of $R_{\mathcal{E}}$ and $d_{\mathcal{E}}$ is the distance between the endpoints a and b.

We note that estimates closely related to those of the next lemma are presented in [4] and [11] for the more general class of John domains. This lemma, in its present form, is given as [7, Lemma 3.6]. It provides an estimate of certain coarse basis functions in our earlier work; it is included here to provide a contrast to Lemma 2.7, which gives a stronger estimate for our new coarse basis functions.

LEMMA 2.5. *Let $\mathcal{E} \in \mathcal{S}_{\mathcal{E}_i}$ with endpoints a and b. There exists an edge function $\vartheta_{\mathcal{E}} \in V^h$ equal to 1 at all nodes of $\mathcal{E}$ and vanishing elsewhere on $\partial\Omega_i$ such that*

$$(\nabla\vartheta_{\mathcal{E}}, \nabla\vartheta_{\mathcal{E}})_{\Omega_i} \leq C(1 + \log(d_{\mathcal{E}}/h_i)), \tag{2.5}$$
$$(\vartheta_{\mathcal{E}}, \vartheta_{\mathcal{E}})_{\Omega_i} \leq Cd_{\mathcal{E}}^2. \tag{2.6}$$

We next introduce a coarse linear interpolant f_ℓ of an arbitrary element $f \in V^h$. The range of this operator will define the coarse subspace of our domain decomposition algorithm and bounds for it will be central in the proof of our main result, which will be based on the abstract Schwarz theory of [13, Chapter 2].

DEFINITION 2.6.   *(Linear Interpolant).   A coarse linear interpolant $f_\ell \in V^h$ of $f \in V^h$ has $f_\ell = f$ at all subdomain vertices of $\partial\Omega_i$. Furthermore, along each subdomain edge $\mathcal{E}$,*

$$\nabla f_\ell \cdot \boldsymbol{t}_i = \frac{f(b) - f(a)}{d_\mathcal{E}} \boldsymbol{d}_\mathcal{E} \cdot \boldsymbol{t}_i$$

where a and b are the endpoints of $\mathcal{E}$ and $d_\mathcal{E}$ is the distance between them. This linear interpolant is a discrete harmonic function in the sense that its values in the interior of the subdomains are obtained by minimizing the norm defined by the bilinear form of (1.2) for given interface values.

Consider an element with an edge $e \subset \mathcal{E}$. For linear finite elements, $\nabla f \cdot \boldsymbol{t}_i$ is constant on e, and the difference in nodal values along this edge is $|e| \nabla f \cdot \boldsymbol{t}_i$, where $|e|$ is the length of the edge. Summing these differences for all elements along $\mathcal{E}$, we find that

$$\int_\mathcal{E} \nabla f \cdot \boldsymbol{t}_i \, ds = f(b) - f(a).$$

The same formula also holds for f_ℓ and we then find that

$$\nabla f_\ell \cdot \boldsymbol{t}_i = \frac{\boldsymbol{d}_\mathcal{E} \cdot \boldsymbol{t}_i}{d_\mathcal{E}} \int_\mathcal{E} \nabla f \cdot \boldsymbol{t}_i \, ds. \tag{2.7}$$

The linear interpolant itself can be expressed in terms of basis functions $\theta_{b\ell}$, which solve interpolation problems with special data. Thus,

$$f_\ell := \sum_{b \in \mathcal{S}_\mathcal{V}} f(b) \theta_{b\ell}. \tag{2.8}$$

LEMMA 2.7.   *(Linear Shape Functions).   There exists a linear interpolant θ_{bl} that vanishes at all subdomain vertices except for b where it equals 1. Further,*

$$(\nabla \theta_{b\ell}, \nabla \theta_{b\ell})_{\Omega_i} \leq C(1 + \log(r_b)), \tag{2.9}$$

where $r_b \geq 1$ is the ratio of the distances between b and its adjacent subdomain vertices a and c.

Proof. We first construct a coarse finite element mesh $\mathcal{T}_{\mathcal{E}_1}$ consisting of a square element containing all of the edge $\mathcal{E}_1$, which connects a and b, and which is surrounded by four trapezoidal elements as shown in Figure 2.2. The square is centered at the midpoint between a and b, and two of its sides are parallel to the line segment between a and b. The length of the side of the square is denoted by $D_{\mathcal{E}_1}$.

The values of a piecewise bilinear function ψ_1 at the top two and bottom two nodes of the internal square equal $1/2 + D_{\mathcal{E}_1}/(2d_{\mathcal{E}_1})$ and $1/2 - D_{\mathcal{E}_1}/(2d_{\mathcal{E}_1})$, respectively, while ψ_1 is chosen to be zero at the remaining four nodes of $\mathcal{T}_{\mathcal{E}_1}$. The function ψ_1 is then extended by 0 to the rest of $\mathbb{R}^2$. By construction, $\psi_1(a) = 0$, $\psi_1(b) = 1$, and $\nabla \psi_1 = (1/d_{\mathcal{E}_1}) \boldsymbol{d}_{\mathcal{E}_1}$ in the internal square element, in which ψ_1, in fact, is a function of just one local coordinate which is defined by

$$x_1 = (\boldsymbol{x} - \boldsymbol{a}) \cdot \boldsymbol{d}_{\mathcal{E}_1}. \tag{2.10}$$
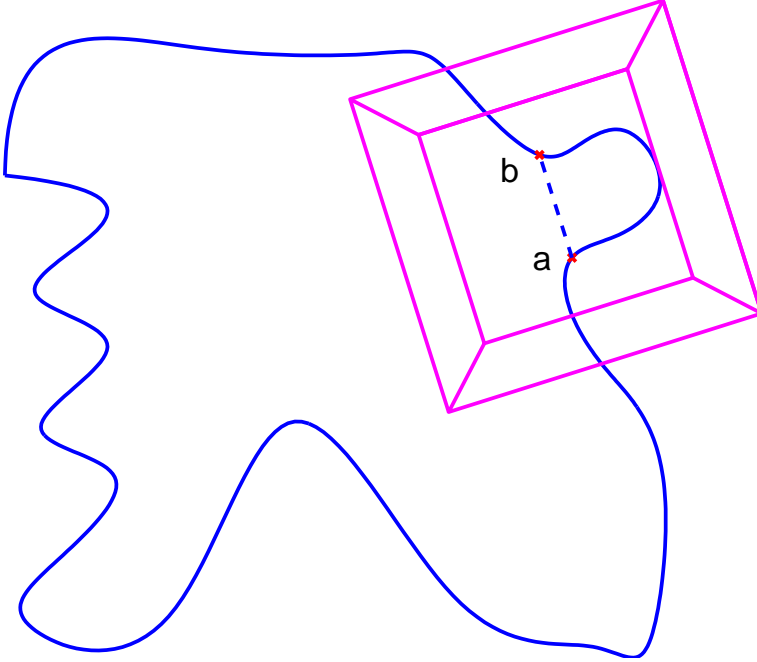
Fig. 2.2. *Coarse mesh $\mathcal{T}_{\mathcal{E}_1}$ around edge $\mathcal{E}_1$ used in the proof of Lemma 2.7. The sides of the internal square element is denoted by $D_{\mathcal{E}_1}$ and the distance from a to b is $d_{\mathcal{E}_1}$. The sides of the assembly of five elements is chosen as $3D_{\mathcal{E}_1}/2$.*

Here $\boldsymbol{x} - \boldsymbol{a}$ is the vector from a to x and $\boldsymbol{d}_{\mathcal{E}_1}$ the unit vector in the direction of $b - a$. With $d_{\mathcal{E}_1}$ the distance between a and b, we see that x_1 varies linearly from 0 at a to $d_{\mathcal{E}_1}$ at b in the direction $\boldsymbol{d}_{\mathcal{E}_1}$ and that $\nabla\psi_1 \cdot \boldsymbol{t}_i = (1/d_{\mathcal{E}_1})\boldsymbol{d}_{\mathcal{E}_1} \cdot \boldsymbol{t}_i$ along $\mathcal{E}_1$. In addition, since $D_{\mathcal{E}_1} \leq Cd_{\mathcal{E}_1}$, by (2.4), and the other four trapezoidal elements are shape regular by construction, it follows that $|\nabla\psi_1|$ is of order $1/d_{\mathcal{E}_1}$ in all five elements. Consequently, since the area of all five elements is of order $d_{\mathcal{E}_1}^2$, we obtain

$$(\nabla\psi_1, \nabla\psi_1)_{\Omega_i} \leq C.$$

We also note that ψ_1 is uniformly bounded.

Let us now denote by $\mathcal{E}_2$ the other edge, between b and c, which also has b as an endpoint. Similarly, $d_{\mathcal{E}_2}$ is the distance between c and b, and a local coordinate x_2 is given by

$$x_2 = (\boldsymbol{x} - \boldsymbol{c}) \cdot \boldsymbol{d}_{\mathcal{E}_2}, \tag{2.11}$$

where $\boldsymbol{d}_{\mathcal{E}_2}$ is the unit vector in the direction $b - c$. We then construct ψ_2 in a way similar to that of ψ_1. We note that ψ_2 goes from 1 to 0 when we move from b to c along the edge $\mathcal{E}_2$; there is a change in sign. Therefore, if we consider the contributions on the edge $\mathcal{E}_1$ from $\nabla\psi_1 \cdot \boldsymbol{t}_i$ and that of the same kind of function corresponding to the vertex a; we will find that they cancel each other. As a result of this observation, we will find that the interpolation formula (2.8) will reproduce any constant.

We will construct a vertex function $\tilde{\theta}_{b\ell}$ which equals 1 at b and vanishes at all other subdomain vertices including a and c. Moreover, $\tilde{\theta}_{b\ell}$ vanishes along all subdomain edges not having b as an endpoint. The values of $\theta_{b\ell}$ in the interior of subdomain

Ω_i are given by the discrete harmonic function defined by the interface data of the finite element interpolant of $\tilde{\theta}_{b\ell}$. In our final estimate, we can use an estimate of the maximum of $|\nabla\tilde{\theta}_{b\ell}|$ over individual elements since the same estimate also holds for its linear interpolant $\theta_{b\ell}$.

Let $\mathcal{E}_3$ denote the edge or union of the edges between c and a which completes $\partial\Omega_i$. Thus, $\partial\Omega_i = a \cup \mathcal{E}_1 \cup b \cup \mathcal{E}_2 \cup c \cup \mathcal{E}_3$. Letting $d_j(x), j = 1, 2, 3$, denote the distance from $x \in \Omega_i$ to $\mathcal{E}_j$, we define a vertex function $\tilde{\theta}_{b\ell}$ by

$$\tilde{\theta}_{b\ell}(x) = \frac{\psi_1(x)/d_1(x) + \psi_2(x)/d_2(x)}{1/d_1(x) + 1/d_2(x) + 1/d_3(x)}. \tag{2.12}$$

It is easy to see that this function is continuous and attains the correct boundary values. It is also uniformly bounded, a fact which we will use in the proof of our main result. An estimate of the energy of its V^h-interpolant will provide an upper bound of the energy of the discrete harmonic function $\theta_{b\ell}$ with the same boundary data.

We obtain, by a direct computation,

$$\nabla\tilde{\theta}_{b\ell} = (\nabla\psi_1 d_1^{-1} + \nabla\psi_2 d_2^{-1} - \psi_1 d_1^{-2}\nabla d_1 - \psi_2 d_2^{-2}\nabla d_2)(d_1^{-1} + d_2^{-1} + d_3^{-1})^{-1} \tag{2.13}$$
$$+ (\psi_1 d_1^{-1} + \psi_2 d_2^{-1})(d_1^{-2}\nabla d_1 + d_2^{-2}\nabla d_2 + d_3^{-2}\nabla d_3)(d_1^{-1} + d_2^{-1} + d_3^{-1})^{-2}.$$

Since $|\nabla d_1| \leq 1$ and $|\nabla d_2| \leq 1$, it follows that

$$|\nabla\tilde{\theta}_{b\ell}| \leq \delta_1|\nabla\psi_1| + \delta_2|\nabla\psi_2| +$$
$$\frac{(1-\delta_3)^2|\psi_2 - \psi_1|}{d_1 + d_2} + \frac{(1-\delta_1)^2|0 - \psi_2|}{d_2 + d_3} + \frac{(1-\delta_2)^2|\psi_1 - 0|}{d_1 + d_3}, \tag{2.14}$$

where

$$\delta_j = \frac{d_j^{-1}}{d_1^{-1} + d_2^{-1} + d_3^{-1}}. \tag{2.15}$$

Since $0 \leq \delta_j \leq 1$, it follows that

$$|\nabla\tilde{\theta}_{b\ell}|^2 \leq 5\left[|\nabla\psi_1|^2 + |\nabla\psi_2|^2 + \frac{(\psi_2 - \psi_1)^2}{(d_1 + d_2)^2} + \frac{\psi_2^2}{(d_2 + d_3)^2} + \frac{\psi_1^2}{(d_1 + d_3)^2}\right]. \tag{2.16}$$

Since $|\nabla\psi_1|$ is of order $1/d_{\mathcal{E}_1}$ and the area of the support of ψ_1 is of order $d_{\mathcal{E}_1}^2$, we see that the integral over Ω_i of the first term on the right hand side of (2.16) is of order 1. The same conclusion also holds for the second term using similar reasoning.

Turning to the remaining three terms, let $d_a(x)$, $d_b(x)$, and $d_c(x)$ denote the distance from $x \in \Omega_i$ to the vertices a, b, and c, respectively. From the definitions of ψ_1 and ψ_2, and the bounds on their gradients, we see that

$$|\psi_2 - \psi_1| \leq Cd_b/\min(d_{\mathcal{E}_1}, d_{\mathcal{E}_2}), \tag{2.17}$$
$$|\psi_2| \leq Cd_c/d_{\mathcal{E}_2}, \tag{2.18}$$
$$|\psi_1| \leq Cd_a/d_{\mathcal{E}_1}. \tag{2.19}$$

We note that, we will need additional arguments when the relative sizes of $d_{\mathcal{E}_1}$ and $d_{\mathcal{E}_2}$ differ considerably. We first assume that they are of the same order of magnitude.

When we estimate the third term of (2.16), we will split Ω_i into two subsets and develop separate bounds for them. Let γ_1 be the curve of Definition 2.1 which

connects b with a and similarly let γ_2 connect b with c. Let x_{γ_1} be the point on γ_1 which is closest to $x \in \Omega_i$ and we then define x_{γ_2} similarly. We also denote by $t_1(x)$ the arc length of the part of the curve γ_1 between b and x_{γ_1} and we then define $t_2(x)$ similarly. We are now ready to define $\Omega_i^b : x \in \Omega_i^b$ if $t_1(x) \leq \ell_1/2$ or $t_2(x) \leq \ell_2/2$ or both. Here, ℓ_1 and ℓ_2 are the lengths of the curves γ_1 and γ_2, respectively. We denote the complement of Ω_i^b by $C\Omega_i^b := \Omega_i \setminus \Omega_i^b$.

By using (2.2), we can now establish a lower bound

$$d_1(x) + \text{dist}(x, \gamma_1) \geq cd_b(x), \text{ for } x \in R_{\mathcal{E}_1} \text{ such that } t_1(x) \leq \ell_1/2,$$

where $c > 0$ is a constant. We note that since $\text{dist}(x, \gamma_1) \leq d_2(x)$, we have a lower bound for $d_1(x) + d_2(x)$. By considering $x \in \Omega_i \setminus R_{\mathcal{E}_1}$ for which $t_1(x) \leq \ell_1/2$ and then, similarly, points in $R_{\mathcal{E}_2}$ and its complement for which $t_2(x) \leq \ell_2/2$, we find that

$$d_1(x) + d_2(x) \geq cd_b(x), \quad \forall x \in \Omega_i^b.$$

The integral of the third term of (2.16) over Ω_i^b is now easily seen to be bounded since for x in that set, we have

$$\frac{(\psi_2 - \psi_1)^2}{(d_1 + d_2)^2} \leq C/(\min(d_{\mathcal{E}_1}, d_{\mathcal{E}_2}))^2. \tag{2.20}$$

We now turn to the task of estimating the integral of the same expression on the left in (2.20) over $C\Omega_i^b$. By quite similar arguments, we can prove that

$$d_1(x) + d_2(x) \geq c\max(d_a(x), d_c(x)), \ x \in C\Omega_i^b.$$

By using (2.18) and (2.19), we then obtain the same estimate for the integrand over $C\Omega_i^b$ and a uniform bound for the integral of that third term over all of Ω_i has then been obtained.

We now outline how we can bound the integral of the fourth term of (2.16); the fifth and final one can be handled quite similarly. We will again work with the curve γ_2 and also with γ_3 which connects c to a. In an appropriate neighborhood Ω_i^c of c, we first develop a lower bound of $d_2(x) + d_3(x)$ in terms of $d_c(x)$. What remains is to obtain a lower bound for $d_2(x) + d_3(x)$ for x in the rest of Ω_i. We recall that when we developed a bound for $x \in C\Omega_i^b$ for the third term, we were able to rely on (2.18) and (2.19), which show that ψ_1 and ψ_2 go to zero linearly when we approach a and b, respectively. In the present context, we write $\psi_2 = (\psi_2 - \psi_1) + \psi_1$ and can then rely on (2.17) and (2.18) and ideas quite similar to those for the third term to obtain a lower bound for $d_2(x) + d_3(x)$ in terms of $\max(d_a(x), d_b(x))$ for $x \in C\Omega_i^c$, where $C\Omega_i^c$ is the complement of Ω_i^c.

If $d_{\mathcal{E}_1}$ and $d_{\mathcal{E}_2}$ are not of the same order of magnitude, we can provide a bound with an additional factor $\log(\max(d_{\mathcal{E}_1}, d_{\mathcal{E}_2})/\min(d_{\mathcal{E}_1}, d_{\mathcal{E}_2})) =: \log(r_b))$. We note that the direct computation of the $H^{1/2}$−norm of the trace of $\theta_{b\ell}$ on $\partial\Omega_i$, for a simple geometry, shows that this logarithmic factor cannot be eliminated.

Let $d_{\mathcal{E}_1} > d_{\mathcal{E}_2}$. The idea is to introduce a number of additional basis functions, in terms of additional vertices on the longer edge. These vertices are found as the last exits y_k by the edge $\mathcal{E}_1$ from circular disks B_k, which are centered at $y_0 := b$ and of radius $2^k d_{\mathcal{E}_2}$. By using Lemma 2.4, we see that on the order of $1 + \log(d_{\mathcal{E}_1}/d_{\mathcal{E}_2})$ circular disks will suffice to cover the entire edge.

A linear basis function can now be constructed for the vertices a, b, and y_1 for which the previous bound is valid. Additional basis functions θ_{y_k} are then constructed

using sets of three consecutive points y_{k-1}, y_k, and y_{k+1} as vertices. Their energy can also be estimated by using the previous bound since, by construction, $|y_{k-1} - y_k|$ is of the same order as $|y_k - y_{k+1}|$. Finally, we note that $\theta_{b\ell}$ can be written as a linear combination of on the order of $1 + \log(d_{\mathcal{E}_1}/d_{\mathcal{E}_2})$ of the new basis functions θ_{y_k}:

$$\tilde{\theta}_{b\ell} = \sum_k c_k \theta_{y_k}$$

where

$$c_k = (\boldsymbol{y}_k - \boldsymbol{a}) \cdot \boldsymbol{d}_{\mathcal{E}_1}/d_{\mathcal{E}_1}.$$

We see that these coefficients are all uniformly bounded by using (2.4).

Finally, we remark that the arguments can be modified so as also to cover the case where a subdomain has only two vertices. $\square$

We will also need a well-known finite element Sobolev inequality, established for John domains in [4, Lemma 3.2].

LEMMA 2.8.

$$\|u - \bar{u}_{\Omega_i}\|_{L^\infty(\Omega_i)}^2 \leq C(1 + \log(H/h))|u|_{H^1(\Omega_i)}^2, \quad \forall u \in V^h(\Omega_i), \tag{2.21}$$

Here $\bar{u}_{\Omega_i}$ denotes the average of u over the subdomain Ω_i. We also have,

$$\|u\|_{L^\infty(\Omega_i)}^2 \leq C(1 + \log(H/h))\|u\|_{H^1(\Omega_i)}^2, \quad \forall u \in V^h(\Omega_i), \tag{2.22}$$

where the full $H^1(\Omega_i)-$norm is defined by

$$\|u\|_{H^1(\Omega_i)}^2 := |u|_{H^1(\Omega_i)}^2 + 1/(H_i)^2\|u\|_{L^2(\Omega_i)}^2.$$

We will now combine this result with that of Lemma 2.7 to obtain the following lemma. It follows after observing that the linear interpolant, defined in Definition 2.6, reproduces constants and by using Lemma 2.2.

LEMMA 2.9. *The linear interpolant f_ℓ of $f \in V^h$ satisfies*

$$(\nabla f_\ell, \nabla f_\ell)_{\Omega_i} \leq C(1 + \log(H_i/h_i))(1 + \log(\max(r_b)))(\nabla f, \nabla f)_{\Omega_i}, \tag{2.23}$$

where C is a constant independent of f.

3. An overlapping Schwarz method and the main result. We will first define our domain decomposition algorithm and then prove our main result, Theorem 3.1.

Our algorithm is a two-level overlapping Schwarz method and we will use a standard result [13, Theorem 2.7] in its analysis. The coarse subspace of our algorithm can be defined as the range of the interpolation operator of Definition 2.6. The local subspaces are defined by $V_i := V^h(\Omega_i') \cap H_0^1(\Omega_i')$. Typically Ω_i' is obtained by repeatedly adding layers of elements to the subdomains Ω_i; see also [6, Section 3.2] for an alternative. The width of the subset of Ω_i that is also covered by neighboring extended subdomains is denoted by δ_i; for a detailed definition, see [13, Assumption 3.1].

As always in the analysis of overlapping Schwarz methods, the main effort in the analysis involves the design and study of a stable decomposition as in [13, Assumption 2.2]. We should provide a bound for a parameter C_0^2 such that

$$a(u_0, u_0) + \sum_{i=1}^N a_i'(u_i, u_i) \leq C_0^2 a(u, u), \quad \forall u \in V^h, \tag{3.1}$$

for some choice of $\{u_i\}_{i=0}^N$, such that

$$u = \sum_{i=0}^{N} R_i^T u_i, \quad u_i \in V_i. \tag{3.2}$$

Here,

$$a_i'(u,v) := \int_{\Omega_i'} \rho \nabla u \cdot \nabla v dx, \quad i \geq 1$$

and R_i^T the injection of V_i into V^h.

Lemma 2.9 provides a bound for $a(u_0, u_0)$ after that we select $u_0 = u_\ell$, the interpolant of u defined by Definition 2.6. The components in the local subspaces $V_i, i \geq 1$, are defined, as in [13, Section 3.6], by $u_i := I^h(\vartheta_i(u - u_0))$, where $\{\vartheta_i\}_{i=1}^N$ is a partition of unity with $0 \leq \vartheta_i \leq 1$, $|\nabla \vartheta_i| \leq C/\delta_i$, and with ϑ_i supported in the closure of Ω_i'. We can choose the $\vartheta_i \in V^h$ and easily prove, by using [13, Lemma 3.9], that $a_j'(u_j, u_j) \leq C a_j'(\vartheta_j(u - u_0), \vartheta_j(u - u_0))$. We will now estimate the latter bilinear form and we will do this by considering the contributions from each subdomain Ω_i, one at a time. In this, we can then equally well work with the $H^1(\Omega_i)$−seminorm and $H^1(\Omega_i)$−norm.

The number of sets Ω_j' that intersect Ω_i is uniformly bounded and we therefore need to consider the contributions from only one of them. We cover $\Omega_j' \cap \Omega_i$ with square patches with sides on the order of δ_i. If the subdomain boundary $\partial \Omega_i$ is Lipschitz, we can do so by using on the order of H_i/δ_i patches. For the more irregular subdomains, considered in this paper, the count can be larger and is related to the Hausdorff dimension of $\partial \Omega_i$; cf., e.g., [8] and also the discussion of this matter in [7, Section 3]. We will denote the patches by π_k and the number of patches needed to cover $\partial \Omega_i$ by $\chi_i H_i/\delta_i$.

By examining a prefractal Koch snowflake curve, a polygonal domain with side length h_i and diameter H_i, we find that $C(4/3)^{\log(H_i/h_i)} H_i/\delta_i$ patches would suffice. In this case, the additional factor $\chi_i \leq C(4/3)^{\log(H_i/h_i)}$ in the count of the number of patches is less than $4 \log(H_i/h_i)$ in the case of a minimal overlap of $\delta_i = h_i$ even in the extreme case of $H_i/h_i = 10^6$.

We observe that $\nabla(\vartheta_j(u - u_0)) = \vartheta_j \nabla(u - u_0) + (u - u_0)\nabla \vartheta_j$. The $L^2(\Omega_i)$−norm of the first of these terms can then immediately be estimated by $|u - u_0|_{H^1(\Omega_i)}$ since $|\vartheta_j| \leq 1$.

To handle the second, we first assume that a maximum principle is valid. This allows us to bound $\|u_0 - \bar{u}_{\Omega_i}\|_{L^\infty(\Omega_i)}$ by $C\|u - \bar{u}_{\Omega_i}\|_{L^\infty(\Omega_i)}$; we use that the coarse basis functions are uniformly bounded on $\partial \Omega_i$ and that $u_0 - \bar{u}_{\Omega_i}$ is the coarse interpolant of $u - \bar{u}_{\Omega_i}$ since the coarse interpolant, defined by (2.8), reproduces constants. By using (2.21), we can estimate the energy contributed by π_k by $C(1 + \log(H_i/h_i))|u|_{H^1(\Omega_i)}^2$ and from all the patches by $C\chi_i H_i/\delta_i(1 + \log(H_i/h_i))|u|_{H^1(\Omega_i)}^2$.

However, a maximum-norm estimate is only available if all angles of the triangulation are acute and it has also not been established for other finite element methods. We will therefore split $u - u_0$ into two terms: $u - u_0 = (u - \tilde{u}_0) + (\tilde{u}_0 - u_0)$. Here $\tilde{u}_0 := \sum_{b \in \mathcal{S}_V} u(b)\tilde{\theta}_{b\ell}$, cf. (2.12), while $u_0 := \sum_{b \in \mathcal{S}_V} u(b)\theta_{b\ell}$. We can now use almost the same argument as before to estimate the L^2−norm of $(u - \tilde{u}_0)\nabla \theta_i$ since, as previously noted, the functions $\tilde{\theta}_{b\ell}$ are uniformly bounded. However, the functions $\tilde{\theta}_{b\ell}$ do not sum to 1 and we therefore have to use (2.22) resulting in a full norm in the right hand side.

What remains is to estimate the L^2- norm of $(\tilde{u}_0 - u_0)\nabla\theta_i$. We use the fact that $\tilde{\theta}_{b\ell} - \theta_{b\ell}$ vanishes on $\partial\Omega_i$ and can be extended by zero to the subset of π_k which is outside Ω_i. This allows us to use Friedrichs' inequality; in fact the argument has been reduced to the case of a square patch with vanishing boundary data on one of its sides. Therefore,

$$\|\tilde{u}_0 - u_0\|^2_{L^2(\pi_k)} \leq C\delta_i^2 |\tilde{u}_0 - u_0|^2_{H^1(\pi_k)}.$$

We can then, after estimating the H^1-seminorm of $\tilde{u}_0$ and u_0, obtain the bound

$$\|(\tilde{u}_0 - u_0)\nabla\theta_i\|^2_{L^2(\Omega_i)} \leq C\chi_i(1 + \max r(b))(1 + \log(H_i/h_i))\|u\|^2_{H^1(\Omega_i)}.$$

As already indicated, we can use Poincaré's inequality replacing the full $H^1(\Omega_i)-$ norm by the $H^1(\Omega_i)-$seminorm, since $u - u_0$ is invariant under a shift by a constant. This completes the proof of our main result:

THEOREM 3.1. *The condition number of our overlapping additive Schwarz algorithm introduced in this section satisfies*

$$\kappa(P_{ad}) \leq C \max_i \left(\chi_i(1 + H_i/\delta_i)(1 + \log(H_i/h_i))\right)(1 + \log(\max(r_b))).$$

The constant C is independent of the number of subdomains, the diameters and meshes of the subdomains as well as of the coefficients ρ_i.

4. Numerical examples. We present some numerical examples in this section to confirm the theory and also to show some advantages of the present coarse space over the one of [4]. The domain for the problem is a unit square discretized by square bilinear elements and subject to homogeneous Dirichlet boundary conditions at the bottom. Preconditioned conjugate gradients is used to solve the associated linear systems to a relative residual tolerance of 10^{-8} for random right-hand-sides. The numbers of iterations and condition number estimates obtained from the conjugate gradient iterations are under the table headings *iter* and *cond*, respectively.

We consider four different types of subdomain decompositions. The first three types are shown in Figure 4.1 and designated by square, ragged, and small-big. We also consider decompositions obtained from a mesh partitioner based on Metis [10]. Some example decompositions obtained from this partitioner are shown in Figure 4.2.

In each of the tables, we compare results from the present coarse space (vertex only) with those from the older one (vertex+edge); we note that the vertex+edge coarse space of [4] has a higher dimension. The number of layers of adjacent elements included in the overlapping subdomains is denoted by the integer n_o. Thus, for a square subdomain of square elements, we have $n_o H_i/\delta_i \approx H_i/h_i$. The results shown in Table 4.1 are for fixed values of $H/h = 8$, $n_o = 2$, and increasing numbers of subdomains N. Results in the top half of the table are for square subdomains, while those in the bottom half are for decompositions from the mesh partitioner. We see in the top half of the table that both coarse spaces lead to scalable algorithms. That is, the condition number estimates are bounded uniformly in terms of N. Interestingly, the vertex only coarse space leads to smaller numbers of iterations and condition number estimates even though its dimension is much smaller than that of the vertex+edge coarse space. Comparing the results in the top and bottom halves of the table, we see that performance is not degraded significantly by using a mesh partitioner for the decomposition.

In Table 4.2, we show the effects of increasing the mesh parameter H/h while holding both the overlap parameter H/δ and the number of subdomains constant.
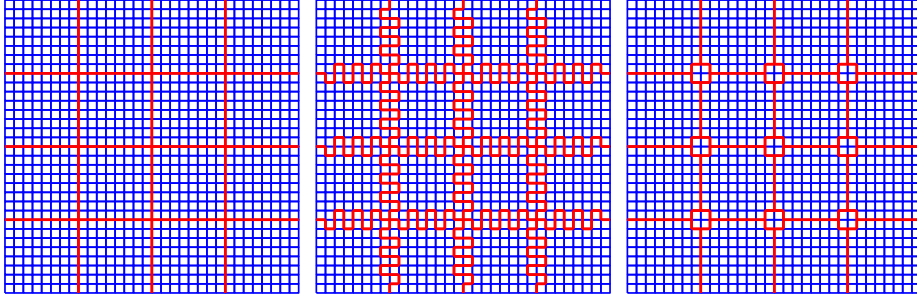
FIG. 4.1. *Examples of square, ragged, and small-big subdomain decompositions.*
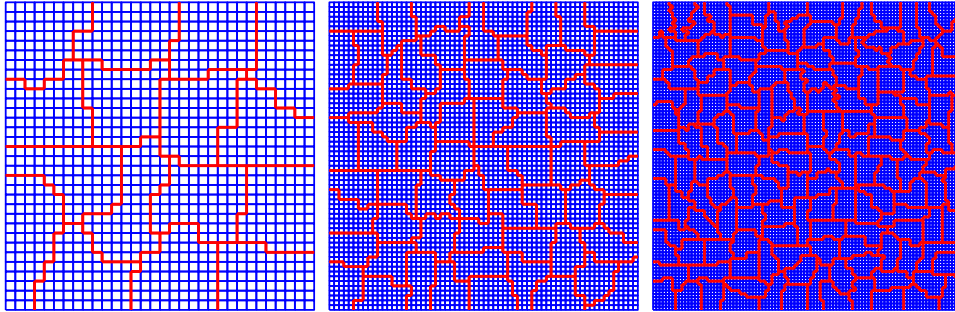
FIG. 4.2. *Example decompositions obtained from a mesh partitioner.*

The results suggest for this problem that condition numbers for the present approach are bounded uniformly with respect to H/h for all three types of decompositions, while those for the richer vertex+edge coarse space exhibit a $\log(H/h)$ dependence.

The original intent for considering small-big mesh decompositions was to exercise the $\log(\max(r_b))$ term in Theorem 3.1 since r_b is proportional to H/h, but the effect of this term was not made evident. We note that, at least for square subdomains, we can make our estimates completely independent of H/h for constant material properties by using a different interpolation formula based on averages of u around a vertex rather than point values; cf. [13, Section 3.5]. As in the previous example, we observe better performance for the new coarse space.

The results in Table 4.3 are for 64 square subdomains with H/δ held fixed and a checkerboard arrangement of material properties. The logarithmic dependence of the condition number is clearly evident for both coarse spaces. In contrast to the previous examples, the vertex+edge coarse space requires fewer iterations and has lower condition number estimates.

For the final example, we consider 64 square subdomains with $H/h = 64$ and different values for the overlap parameter n_o. The results in Table 4.4 are consistent with the linear dependence on H/δ of the condition number estimate in Theorem 3.1.

TABLE 4.1

Results for unit square domain decomposed into N subdomains, each with approximately $(H/h)^2 = 64$ elements. Subdomain material properties are constant with $\rho_i = 1$, and the coarse space dimension is denoted by n_c.

N	vertex only			vertex+edge		
	n_c	$iter$	$cond$	n_c	$iter$	$cond$
square subdomains						
16	18	20	5.3	33	26	9.1
64	70	21	5.4	161	29	9.9
144	154	21	5.5	385	30	10.1
256	270	21	5.5	705	30	10.2
mesh partitioner subdomains						
16	27	23	5.8	49	30	10.2
64	115	25	6.0	244	34	10.5
144	274	27	7.1	612	38	13.6
257	490	29	8.3	1107	39	13.9

TABLE 4.2

Results for unit square domain decomposed into 64 subdomains with $H/\delta = 4$ held constant. Subdomain material properties are constant with $\rho_i = 1$.

H/h	vertex only		vertex+edge	
	$iter$	$cond$	$iter$	$cond$
square subdomains				
8	21	5.4	29	9.9
16	21	5.5	33	12.2
32	22	5.5	36	14.6
64	22	5.5	39	17.0
ragged subdomains				
8	25	6.5	37	16.5
16	23	5.6	40	19.1
32	22	5.3	42	21.7
64	23	5.3	43	24.1
small-big subdomains				
8	24	6.4	28	9.5
16	24	6.7	33	12.2
32	24	6.8	37	14.8
64	25	6.9	41	17.5

TABLE 4.3

Results for unit square domain decomposed into 64 square subdomains with $H/\delta = 4$ held fixed. The material properties are in a checkerboard arrangement with black squares having $\rho_i = 1$ and red squares having $\rho_i = 10^3$.

H/h	vertex only		vertex+edge	
	$iter$	$cond$	$iter$	$cond$
8	32	13.8	27	8.4
16	34	16.2	30	10.0
32	36	18.6	31	11.5
64	37	20.8	34	13.0

TABLE 4.4

Results for unit square domain decomposed into 64 square subdomains with $H/h = 64$ held fixed.

n_o	vertex only		vertex+edge	
	$iter$	$cond$	$iter$	$cond$
1	55	45.8	71	73.4
2	41	23.9	59	36.4
3	35	16.6	52	27.4
4	31	13.0	48	23.7

REFERENCES

[1] Manoj Bhardwaj, Garth Reese, Brian Driessen, Kenneth Alvin, and David Day. Salinas - an implicit finite element structural dynamics code developed for massively parallel platforms. In *41st AIAA/ASME/ASCE/AHS/ASC SDM April 3-6, 2000/Atlanta, GA*, AIAA 2000-1651, 2000.

[2] Stephen M. Buckley and Pekka Koskela. Sobolev-Poincaré implies John. *Math. Res. Lett.*, 2(5):577–593, 1995.

[3] Clark R. Dohrmann, Axel Klawonn, and Olof B. Widlund. Extending theory for domain decomposition algorithms to irregular subdomains. In Ulrich Langer, Marco Discacciati, David Keyes, Olof Widlund, and Walter Zulehner, editors, *Proceedings of the 17th International Conference on Domain Decomposition Methods in Science and Engineering, held in Strobl, Austria, July 3-7, 2006*, number 60 in Springer-Verlag, Lecture Notes in Computational Science and Engineering, pages 255–261, 2007.

[4] Clark R. Dohrmann, Axel Klawonn, and Olof B. Widlund. Domain decomposition for less regular subdomains: Overlapping Schwarz in two dimensions. *SIAM J. Numer. Anal.*, 46(4):2153–2168, 2008.

[5] Clark R. Dohrmann and Olof B. Widlund. An overlapping Schwarz algorithm for almost incompressible elasticity. *SIAM J. Numer. Anal.*, 47(4):2897–2923, 2009.

[6] Clark R. Dohrmann and Olof B. Widlund. Hybrid domain decomposition algorithms for compressible and almost incompressible elasticity. *Internat. J. Numer. Meth. Engng.*, 82:157–183, 2010.

[7] Clark R. Dohrmann and Olof B. Widlund. An iterative substructuring algorithm for two-dimensional problems in H(curl). Technical Report TR2010-936, Department of Computer Science, Courant Institute of Mathematical Sciences, New York University, November 2010.

[8] Kenneth Falconer. *Fractal Geometry: Mathematical Foundations and Applications*. John Wiley & Sons Inc., Hoboken, NJ, second edition, 2003.

[9] Peter W. Jones. Quasiconformal mappings and extendability of functions in Sobolev space. *Acta Math.*, 147(1-2):71–88, 1981.

[10] George Karypis and Vipin Kumar. *METIS Version 4.0*. University of Minnesota, Department of Computer Science, Minneapolis, MN, 1998.

[11] Axel Klawonn, Oliver Rheinbach, and Olof B. Widlund. An analysis of a FETI–DP algorithm on irregular subdomains in the plane. *SIAM J. Numer. Anal.*, 46(5):2484–2504, 2008.

[12] Vladimir G. Maz'ja. Classes of domains and imbedding theorems for function spaces. *Soviet Math. Dokl.*, 1:882–885, 1960.

[13] Andrea Toselli and Olof Widlund. *Domain Decomposition Methods - Algorithms and Theory*, volume 34 of *Springer Series in Computational Mathematics*. Springer-Verlag, Berlin Heidelberg New York, 2005.